NANO LETTERS

2007
Vol. 7, No. 3
583−587

Effect of Nanoscale Curvature of Single-Walled Carbon Nanotubes on Adsorption of Polycyclic Aromatic Hydrocarbons

Suzana Gotovac, Hiroaki Honda, Yoshiyuki Hattori, Kunimitsu Takahashi,† Hirofumi Kanoh, and Katsumi Kaneko*

Graduate School of Science and Technology, Chiba University, 263-8522 Yayoi, Chiba, Japan, and Laser Institute Center, Institute of Research and Innovation, Kashiwa 277-0861, Chiba, Japan

Received September 25, 2006; Revised Manuscript Received February 6, 2007

ABSTRACT

Liquid-phase adsorption of tetracene and phenanthrene on a single-walled carbon nanotube (SWCNT) was examined. Tetracene adsorption was more than six times greater than that of phenanthrene. X-ray photoelectron spectroscopic examination clearly showed that tetracene and phenanthrene molecules efficiently coated the SWCNT external surfaces. The remarkable difference between the adsorption amounts of tetracene and phenanthrene was caused by the nanoscale curvature effect of the tube surface, resulting in a difference in the amount of contact between the molecule and the tube surface. The adsorption of tetracene and phenanthrene caused a significant higher frequency shift in the radial breathing mode (RBM) of the Raman band of the SWCNT, indicating an intensive π–π interaction between these polycyclic aromatic hydrocarbons and the external SWCNT surface.

A single-walled carbon nanotube (SWCNT) is composed of a single graphene tube and caps, and it has a surface-sensitive nature.[1−2] New methods that can control the physical properties of SWCNTs (electronic, optical, magnetic, thermal, mechanical, and chemical, etc. properties) are needed in order to be able to develop their potential applications. Because the graphene tube structure is an array of carbon hexagons with a π-electronic structure similar to that of a polynuclear aromatic hydrocarbon (PAH) molecule, coating of SWCNTs' surfaces with PAH molecules may be one property control method. The adsorption of PAH molecules from solution, as performed in our study, has the advantage in the surface control of isolated SWCNTs of tracking the chirality or the noncovalent functionalization. For example, a theoretical study by Zhao et al.,[3] suggested that coupling between π-electrons in SWCNTs and aromatic molecules can cause changes in the electronic properties of a carbon nanotube. There are gas-phase and liquid-phase adsorption routes for coating of SWCNTs with PAH molecules. The bundles can be untied and the PAH molecules' coverage can be carefully regulated to show the SWCNTs coverage-dependent properties in the case of liquid-phase adsorption. Hence, liquid-phase adsorption may be a better way to coat the SWCNT surface with PAH molecules. However, we must, take into account an inherent point in the adsorption of PAH molecules on a SWCNT surface. In contrast to adsorption on a basal plane of graphite where PAH molecules are known to adsorb laying flat (face-to-face),[4−6] the PAH molecules' molecular surface contact area with the curved tube wall of the SWCNT decreases markedly with a decrease in the tube's diameter. It is essential to explain the effect of an SWCNT's nanoscale curvature on the surface coating. The smallest molecular widths of linear PAH molecules such as naphthalene and tetracene are slightly less than 1 nm. Hence, the molecular geometry of PAH molecules is critical to the adsorption on SWCNTs of 1−2 nm in diameter. We describe the adsorption of PAH molecules of different geometry and size on SWCNTs with a nanoscale radius tube curvature. Phenanthrene and tetracene molecules from toluene solutions were adsorbed on SWCNT samples with mostly closed caps, and the adsorbed state of the PAH molecules on the SWCNTs' surfaces was examined using Raman resonance spectroscopy and X-ray photoelectron spectroscopy (XPS).[7−11] We expected the radial breathing mode (RBM) of the Raman spectrum to be sensitive to the adsorption coating of the nanotubes with PAH molecules.

The SWCNT samples were produced using the laser ablation method with Ni and Co as catalysts at 1423 K. The

* To whom correspondence should be addressed. E-mail: kaneko@pchem2.s.chiba-u.ac.jp. Telephone: ++81-43-290-2779. Fax: ++81-43-290-2788.

† Laser Institute Center, Institute of Research and Innovation.

10.1021/nl0622597 CCC: $37.00
Published on Web 02/23/2007

SWCNTs were treated with 15% hydrogen peroxide and heated at 373 K for 35 min. Thermogravimetry revealed that only 4% of the catalyst metal remained and there was virtually no amorphous phase. The Raman spectra were measured using a 532 nm frequency-doubled Nd:YAG laser (1.8 mW). The initial RBM of as-purified SWCNTs showed two peaks at 185 and 165 cm^{-1}, which, using the Kataura plot, corresponded to diameters of 1.35 and 1.50 nm, respectively.[12−14] D-band intensity was almost nondetectable, confirming that the quantity of the amorphous phase in the sample was negligible. The nitrogen adsorption isotherm gave 382 m^2/g of specific surface area, which is a characteristic value of SWCNT bundles with mostly closed caps and very few nanowindow openings. These characterization results are shown in the Supporting Information.

Adsorption isotherms of tetracene and phenanthrene from toluene solution were measured on SWCNTs dispersed by ultrasonication. The absolute quantities of the PAH molecules in the solutions were regulated to less than the monolayer adsorption on the SWCNTs' surfaces. We first approximated the total surface area of isolated SWCNTs to be around 1890 m^2/g.[15] Vials containing SWCNTs soaked in PAH solutions of different concentrations were ultrasonicated and equilibrated in a shaker bath at 293 K and 100 rpm. The concentration difference of PAH in the solution measured by UV−vis spectrophotometry before and after adsorption was used to determine the adsorption isotherms. Adsorption coating of SWCNTs with pentacene was carried out additionally, although we could not determine the adsorption isotherm because the solubility of pentacene in toluene was too low. We expected pentacene to interact strongly with SWCNT.[16−18] In all cases, the SWCNTs were filtrated from equilibrated solution and later examined in a dried state using XPS and Raman resonance spectroscopy. The XPS experimental conditions were the same for all samples and were as follows: acceleration tension 10 kV, emission current 10 mA (Mg Kα X-ray source), room temperature, and vacuum 10^{-7} Pa. Raman spectroscopy conditions were performed under the same conditions as the Raman measurements in the above characterization part.

Adsorption isotherms of phenanthrene and tetracene are shown in Figure 1. Remarkably different adsorption behavior was observed. The amount of phenanthrene adsorbed (50 mg/g) is very small compared with the adsorbed amount of tetracene. This remarkable difference may be associated with the molecular size and geometry difference between the molecules. Tetracene is a long four-ring molecule with a large π-electron system, which makes it more suitable for adsorption by $\pi-\pi$ interactions along the nanotube axis than phenanthrene.

Figure 2 shows the contact model of phenanthrene, tetracene, and pentacene with the surface SWCNT (diameter 1.5 nm) under the assumption that the molecular axis aligns with the tube axis. The tube model was (13,9), a chiral nanotube that was calculated to be the most likely type of nanotube to correspond to a predominant RBM peak of 185 cm^{-1}. As the phenanthrene molecule does not have a simple rectangular structure, it cannot make flush contact with the

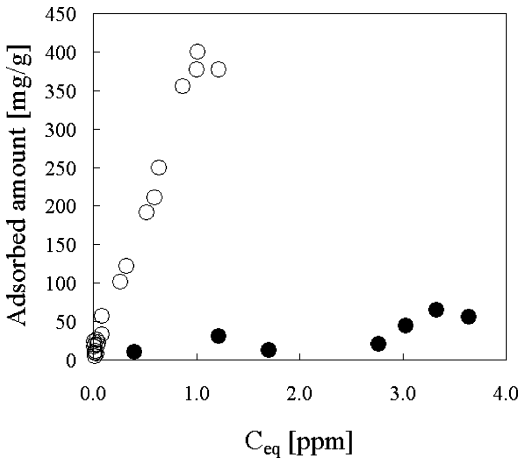

Figure 1. Adsorption isotherms of phenanthrene (●) and tetracene (○) from toluene solution on SWCNTs.

curved SWCNT surface. On the other hand, tetracene can make a good contact with the SWCNT surface. The level of contact between the molecule and tube surface gives an indication of the strength of the $\pi-\pi$ interaction. The aromatic ring number of the two PAH molecules contacting with the SWCNT surface is as follows: 4 rings for tetracene and 2.5 for phenanthrene. Therefore, the adsorption amount difference is probably due to the $\pi-\pi$ contact difference between the molecules.

We confirmed the adsorption coatings using X-ray photoelectron spectroscopy. Figure 3 shows the C1s spectral change with surface coverage. The spectra of the as-purified SWCNTs show a typical graphite peak at 284 eV, while the peaks of pure phenanthrene and tetracene are situated on the higher binding energy side. The progressive appearance of the peaks on the higher binding energy side as well as the disappearance of the graphite peak after surface coverage can be observed. This is clear evidence of surface coating of the external SWCNT surface with PAH molecules. A strong interaction between the SWCNT surface and these PAH molecules was confirmed using Raman spectroscopy.

The Raman RBM band on PAH-adsorbed SWCNTs in a dry state was measured to understand the adsorbed state of PAH molecules. Figure 4 shows changes in the Raman RBM spectra of SWCNTs containing different amounts of the three adsorbates. Here, the adsorption amount is shown in terms of the surface coverage, which is derived from the adsorbed amount, molecular surface area, and specific surface area of the SWCNTs, assuming that the adsorption was face-to-face adsorption (1.98×10^{-18} m^2 phenanthrene and 2.49×10^{-18} m^2 tetracene). A clear higher frequency shift of the peak at 185 cm^{-1} was observed in both cases. The peak at 165 cm^{-1} disappears with the adsorption of phenanthrene and tetracene even at a low coverage rate. At the same time, the G- and D-bands did not change. Consequently, this marked change is inherent to the RBM mode. On average, the shift of the 185 cm^{-1} peak was 8 cm^{-1}. The extinction of the 165 cm^{-1} peak was also confirmed in the pentacene-adsorption treated sample (Supporting Information).

Recently, Zhang et al.[19] reported that individual nanotubes layered on silicon wafer substrate are influenced by the

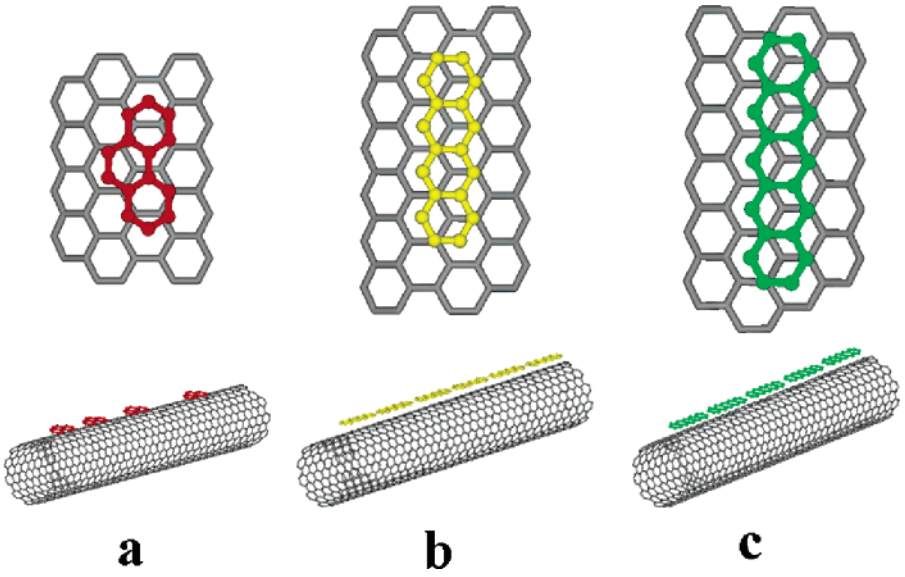

Figure 2. Adsorption models of PAH molecules on SWCNTs ((a) phenanthrene, (b) tetracene, and (c) pentacene). PAH molecules are assumed to be adsorbed in the way that the molecular axis is parallel to the nanotube axis.

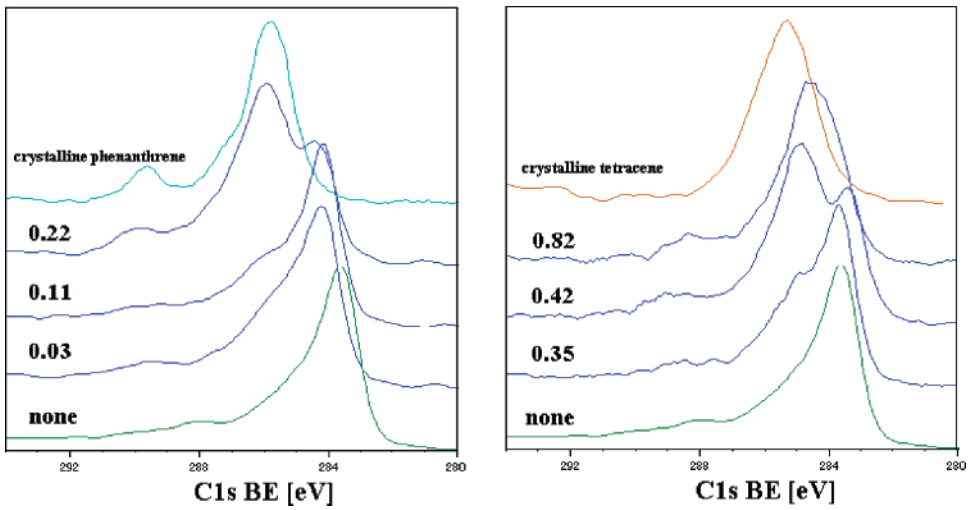

Figure 3. XPS C1s spectra of adsorption-treated samples compared to those of as-purified SWCNTs and pure crystalline adsorbate molecules ((a) phenanthrene, (b) tetracene) as a function of the surface coverage.

"mode hardening effect", resulting in a higher frequency shift in the RBM bands. The change we observed in RBM bands after adsorption treatment also induced a higher frequency shift. Therefore, the $\pi-\pi$ interactions between SWCNTs and PAH molecules probably give rise to a kind of "mode hardening effect". In particular, the higher frequency shift indicates that SWCNTs becomes stiffer after coating with PAH molecules. If the shift would increase with number of π-electrons, adsorption of tetracene is expected to induce a more remarkable shift because of the better molecule−SWCNT contact. However, the observed shifts for tetracene and phenanthrene adsorption were almost the same. In the experimental coverage range, these PAH molecules should coat the surface of SWCNTs well, inducing the observed higher frequency shift. Numerous theoretical studies on the stability of benzene molecules on SWCNT[3,20−22] support the above explanation. The most favorable adsorption states of phenanthrene and tetracene molecules on SWCNT (or graphite) should be the so-called "bridge positions" like in the preceding benzene on SWCNT case.[3] Figure 5a illustrates this position as the case of adsorption on the ideally flat graphite surface. The π-orbitals are slightly mismatched due to the repulsion of the negative charges. At the same time, hydrogen atoms in the PAH molecules are attracted by the negatively charged π-systems inducing the "bridge" position. The SWCNTs used in this study were mostly semiconducting according to the shape of the G−D band (Supporting Information). We selected the typical semiconducting chiral (n,m = 13,9) nanotube for a model and have shown the possible "bridge" positions of PAH molecules aligned along the nanotube axis in Figure 5b. Obviously, every single PAH molecule is likely to disturb the radial flexibility of a significant number of the aromatic rings in the tube structure, causing the hardening of the RBM mode. This explains why the RBM shifts were very marked, even at the relatively low

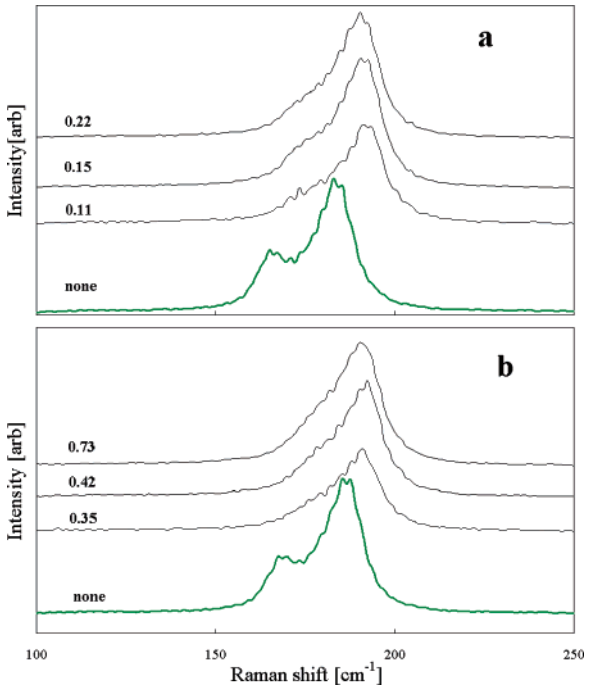

Figure 4. Raman RBM spectral changes of SWCNTs adsorbing PAHs with the surface coverage of the SWCNTs by PAH molecules ((a) phenanthrene, (b) tetracene).

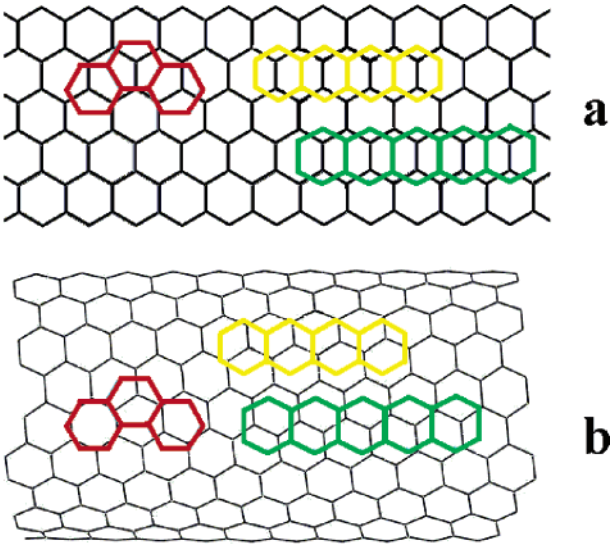

Figure 5. Plausible adsorbed states of phenanthrene and tetracene molecules on the basal plane of graphite (a) and on (n,m = 13,9) chiral SWCNT (b) surfaces (red, phenanthrene; yellow, tetracene; green, pentacene). Hydrogen atoms are omitted for clarity.

coverage rate of 0.1 in the case of phenanthrene. The shift may be saturated above this coverage.

Our results show that the diameter-dependent nanoscale curvature must be taken into account when considering the adsorption treatment of carbon nanotubes for various applications. At the same time, the adsorbed amount depends heavily on the extent of the π-electron-conjugated system of organic molecules adsorbed on SWCNTs, while the hardening of the tube structure can be observed even at lower coverage. A preliminary X-ray diffraction study of the SWCNTs adsorption-treated under the conditions of the mass ratios in solutions of 2:1 = tetracene/SWCNT showed a remarkable expansion of the intertubular spacing by 0.77 nm, corresponding to the bilayer thickness of a tetracene molecule (Supporting Information, Figures S4 and S5). A more systematic study for pillaring of the SWCNT bundles with PAH molecules is needed to design highly porous SWCNT bundles of characteristic electronic properties.

Acknowledgment. We thank the Center of Excellence (COE), Chiba University, who granted S.G. the scholarship. The experimental part of the research was funded by Japanese Government's Grant-in-Aid for Scientific Research (S). We are grateful to Kouki Urita for the help with illustrations.

Supporting Information Available: Scanning electron microscope image of purified LA-SWCNTs and tetracene adsorbed sample (Figure S1). Raman spectrum of the as-purified SWCNTs at higher frequencies, G- and D-band (Figure S2). Nitrogen adsorption isotherm on the as-purified SWCNTs samples (Figure S3). RBM of the pentacene adsorption-treated sample (Figure S4). XRD patterns of the as-purified and tetracene adsorption-treated SWCNT samples (inset: wide-scale XRD pattern of as-purified SWCNT with intertubular peak marked) (Figure S5). Difference XRD patterns of the tetracene adsorption-treated sample and as-purified SWCNT samples (Figure S6). This material is available free of charge via the Internet at http://pubs.acs.org.

References

(1) Romero, H. E.; Bolton, K.; Rosén, A.; Eklund, P. C. *Science* **2005**, *307*, 89.
(2) Urita, K.; Seki, S.; Utsumi, S.; Noguchi, D.; Kanoh, H.; Tanaka, H.; Hattori, Y.; Ochiai, Y.; Aoki, N.; Yudasaka, M.; Iijima, S.; Kaneko, K. *Nano Lett.* **2006**, *6*, 1325.
(3) Zhao, J.; Lu, J. P. *Appl. Phys. Lett.* **2003**, *82*, 3746.
(4) Zhu, D.; Pignatello, J. J. *Environ. Sci. Techonol.* **2005**, *39*, 2033.
(5) Florio, G.; Werblowsky, T. L.; Muller, T.; Berne, B. J.; Flynn, G. W. *J. Phys. Chem B* **2005**, *109*, 4520.
(6) O'Dea, A. R.; Smart, R. St. C.; Gerson, A. R. *Carbon* **1999**, *37*, 1133.
(7) Freitag, M.; Martin, Y.; Misewich, J. A.; Martel, R.; Avouris, Ph. *Nano Lett.* **2003**, *3*, 1067.
(8) Jorio, A.; Pimenta, M. A.; Souza, Filho, A. G.; Saito, R.; Dresselhaus, G.; Dresselhaus, G. M. *New J. Phys.* **2003**, *5*, 139.
(9) Kataura, H.; Kumazawa, Y.; Maniwa, Y .; Umezu, I.; Suzuki, S.; Ohtsuka, Y.; Achiba, Y. *Synth. Met.* **1999**, *103*, 2555.
(10) Alvarez, L.; Righi, A.; Guillard, T.; Rols, S.; Anglaret, E.; Laplaze, D.; Sauvajol, J.-L. *Chem. Phys Lett.* **2000**, *316*, 186.
(11) Weisman, R. B.; Bachilo, S. M. *Nano Lett.* **2003**, *3*, 1235.
(12) Strano, M. S.; Doorn, S. K.; Haroz, E. H.; Kittrell, C.; Hauge, R. H.; Smalley, R. E. *Nano Lett.* **2003**, *3*, 1091.
(13) Saito, R.; Dresselhaus, G.; Dresselhaus, M. *Physical Properties of Carbon Nanotubes*; Imperial College Press: London, 1998.
(14) Samsonidze, G. G.; Saito, R.; Kobayashi, N.; Gruneis, A.; Jiang, J.; Jorio, A.; Chou, S. G.; Dresselhaus, G.; Dresselhaus, M. S. *Appl. Phys. Lett.* **2004**, *85*, 5703.
(15) Williams, K. A.; Eklund, P. C. *Chem. Phys. Lett.* **2000**, *320*, 352.
(16) Nakamura, M.; Ohguri, H.; Yanagisawa, H.; Goto, N.; Ohashi, N.; Kudo, K. Proceedings of the International Symposium on Super-Functionality Organic Devices; IPAP Conference Series 6; Institute of Pure and Applied Physics: Tokyo, 2005; p 130.
(17) Wang, L.; Fine, D.; Jung, T.; Basu, D.; Von Seggern, H.; Dodabalapur, A. *Appl. Phys. Lett.* **2004**, *85*, 1772.

(18) Qi, P.; Javey, A.; Rolandi, M.; Wang, Q.; Yenilmez, E.; Dai, H. *J. Am. Chem. Soc.* **2004**, *126*, 11774.
(19) Zhang, Y.; Zhang, J.; Son, H.; Kong, J.; Liu, Z. *J. Am. Chem. Soc.* **2005**, *127*, 17156.
(20) Tournous, F.; Latil, S.; Heggie, M. I.; Charlier, J.-C. *Phys. Rev. B* **2005**, *72*, 075431.
(21) Lu, J.; Nagase, S.; Zhang, X.; Wang, D.; Ni, M.; Maeda, Y.; Wakahara, T.; Nakahodo, T.; Tsuchiya, T.; Akasaka, T.; Gao, Z.; Yu, H.; Mei, W. N.; Zhou, Y. *J. Am. Chem. Soc.* **2006**, *128*, 5114.
(22) Veiga, R. G. A.; Miwa, R. H. *Phys. Rev. B* **2006**, *73*, 245422.

NL0622597